New generation of lead-free solder alloys with high thermal reliability for applications in harsh environments

Jie Geng, Ph.D. and Hongwen Zhang, Ph.D.
Indium Corporation
Clinton, NY 13413
e-mail: jgeng@indium.com

I. INTRODUCTION

Lead-free solder alloys have been widely adopted by the electronics industry since the Restrictions on Hazardous Substances (RoHS) regulations were implemented in the European Union in July 2006. In the past decades, lead-free SnAgCu ("SAC") solder alloys such as Sn3.0Ag0.5Cu (SAC305) and Sn3.8Ag0.7Cu (SAC387) have been used extensively in portable, computing, and mobile electronics, which operate in temperatures of 125°C and below. Automotive electronics must operate in temperatures around 150°C for under-the-hood devices and below 125°C for devices in the passenger compartment. These electronics must also be able to function in very low temperatures, requiring an operational range of -40°C to +150°C.

For such harsh environments, the traditional binary or ternary lead-free Sn-rich solder alloys are not reliable enough to survive. Relative to the melting temperature of most Sn-rich solders, the homologous temperature at 150°C equals to 0.876 for SnAgCu-3Bi, 0.863 for SnAgCu, 0.856 for Sn-3.5Ag and 0.846 for Sn-0.7Cu, indicating that atomic diffusion will facilitate microstructural evolution and accelerate joint degradation. Higher operating temperatures result in increased rates of microstructural coarsening and joint degradation. The disclosed high-reliability solders for higher-service-temperature applications reflect consideration of metallurgical designs to approach environmental performance issues. These designs slow down the microstructural evolution of the joint solder body and interfacial intermetallic compound (IMC) growth originating from atomic diffusion under thermal migration, which in return maintains the joint fatigue resistance.

In addition to temperature, automotive electronics need to survive continuous vibration and mechanical shocks during vehicle movement and braking. Ductile joints are desired because of their improved vibration/shock resistance. However, interfacial IMC growth and microstructural evolution render the joint more brittle, especially at higher temperatures. Thus, it is desirable to design a ductile joint sustainable during operation under harsh conditions.

High-temperature and high-reliability Sn-rich solder can be used for high-brightness (HB) LED chip module assembly and die-attachment in power semiconductor modules. For power semiconductor modules, the joule heat generated from the loaded electrical current will increase the joint junction temperature to 150°C or even higher, depending on the module design. Higher current densities cause increased joint temperatures if the heat-dissipation method remains the same. During operation, the HB-LED will heat the joints (both the anode and cathode joints as well as the thermal pad joint between the two electrodes) up to 150°C or even higher rapidly depending on the operational electrical current and the cooling pad design, similar to that in power modules. The transit heat in the high-power devices, including both HB-LED and power modules, would severely stress the bonding joint. Thus, the design of the high-reliability solder for power devices must improve the joint resistance to both current and thermal stressing, which can be implemented by controlling the atomic diffusion under both electro-migration and thermal migration.

To address the need for solder materials for the automotive industry and power devices, novel metallurgical designs for high-reliability lead-free solders focus on stabilizing the microstructural evolution and slowing down the interfacial IMC growth under both thermal and current stressing conditions.

II. ENHANCED RELIABILITY BY ANTIMONY ADDITION

In the recent development of high-performance lead-free solder alloys, antimony (Sb) plays a key role in improving the thermal fatigue resistance of solder joints in harsh thermal cycling or thermal shock conditions. According to the binary Sn-Sb phase diagrams [1, 2], the solubility of Sb in Sn is approximately 0.5 wt. % at room temperature and about 1.5 wt. % at 125°C. Solid solution strengthening is thus expected in these alloys due to the dissolution of Sb in Sn-based lead-free solders [3].

Alloying with Sb (1.5-9.0wt%) has showed different thermal fatigue resistances [1]. The fine SnSb IMC particles nucleate and grow into nano/micron-sized clusters under certain stoichiometric ratios after reflow solidification. These in-situ SnSb particles inside Sn matrix could be reversely dissolved back to form a solid solution under high temperatures and then precipitate out again after cooling down. Sufficient Sb is required to strengthen the solder alloy with both solid-solution and precipitation [4]. When Sb is reduced below 3.0 wt%, fine SnSb particles are completely dissolved back into the Sn matrix to form a Sn-Sb solid solution if serving at 150°C and above; no SnSb fine particles remain to strengthen the alloy. Strengthening in alloys is associated with interrupting the dislocation movement. Both fine particles embedded in the alloy matrix and solute atoms in the solid solution act as obstacles to inhibit the dislocation slide along the favorable lattice directions. Atomic diffusion favors dislocation movement at high temperatures (homologous temperature > 0.6). For small obstacles like

solute atoms, atomic diffusion can easily assist the dislocation to bypass or "climb over" obstacles. For large obstacles like precipitates, more atomic diffusion steps are needed to allow the dislocations to bypass the obstacles. Thus, precipitates are more effective to maintain high-temperature strength through interfering dislocation movements.

Therefore, 4.5 wt% and more Sb is expected to strengthen the alloys with sufficient precipitates, even above 150°C. However, above 10 wt% of Sb addition, the solder alloys will have a liquidus temperature above 266°C, making it challengeable to be reflowed well with the conventional SAC305 process (the peak reflow temperature is usually below 245°C). The optimal Sb content balancing the strengthening and the reflow was found to be at 5.5 wt.% [4–6]. This led to the development of the 90.6Sn-3.2Ag-0.7Cu-5.5Sb (Indalloy®276) high-reliability solder alloy [4].

It has also been reported that Sb slows the growth rate of the interfacial Cu_6Sn_5 IMC [5, 7, 8]. Figure 1 shows the relative growth rate of IMC thickness in SMR0805-resistor joints of the SAC305 and Indalloy®276 during thermal cycling of -40/125°C. The relative growth rate was calculated based on interfacial IMC thickness of 0 cycle. Before the thermal cycling test, the IMC layer thickness in both SAC305 and Indalloy®276 was very close—1.51 and 1.62µm, respectively. After 2000 cycles, the IMC layer in SAC305 grew more than 60% to 2.48µm, nearly tripling the Indalloy®276 growth. Furthermore, between 2000 and 3000 cycles, the IMC layer in SAC305 grew significantly to 170% greater than its value at 0 cycles, while the Indalloy®276 only grew to 70% relative to its starting thickness. Fast interfacial IMC growth on Cu surfaces tends to produce irregular and non-uniform IMC layers. This can lead to reduced mechanical reliability by inducing fractures at IMC interfaces or through the IMC in-drop shock loading [9].

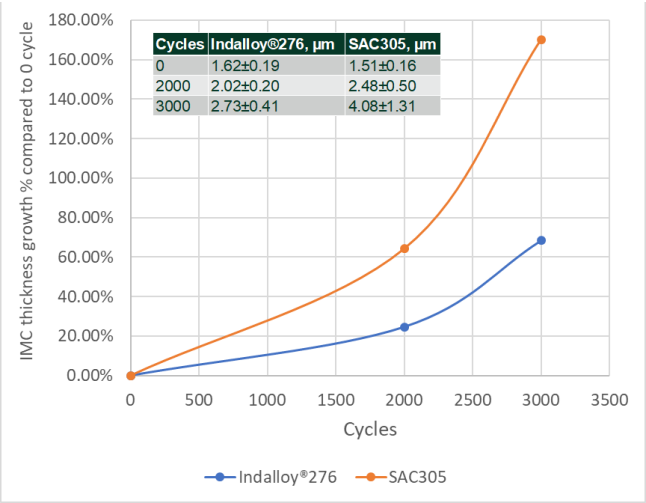

Figure 1. The IMC layer thickness growth rate (compared to zero cycle) in SMR0805 resistors (on ImSn surface finish) of SAC305 and Indalloy®276 at 2000 and 3000 cycles under thermal cycling of -40/125°C.

Figure 2 shows the calculated crack ratios in the joints (SMR0805 resistor on ImSn surface finish) at various intervals of thermal cycling under -40/125°C. The crack ratio after 3000 cycles was more than 70% in SAC305 while only 23% in Indalloy®276. The crack resistance is much improved in Indalloy®276 compared to SAC305. The observations displayed in Figures 1 and 2 indicate that alloying with Sb may improve thermal fatigue performance through slowing the IMC growth apart from the solid solution strengthening and precipitation hardening mechanisms.

Presumably, the mechanisms involve solid solution strengthening and precipitation hardening, as well as the positive effect brought by Sb to slow down the IMC layer growth. To obtain optimal strengthening, the Sb content was set to 5.5 wt.% to provide enough Sb to have solid solution strengthening and precipitation hardening. This mass density of Sb may cause the alloy to reach an optimal volume fraction of micro-sized SnSb intermetallic precipitates, which are reported by Lu, et al. [10] and El-Daly, et al. [11] to be distributed throughout the Sn dendrites. In this case, the SbSn precipitates form within the Sn dendrites, unlike the well-known SAC Ag_3Sn mechanism where the precipitates form at the Sn dendrite boundaries. The SbSn precipitates appear to resist recrystallization by strengthening the Sn dendrites [12].

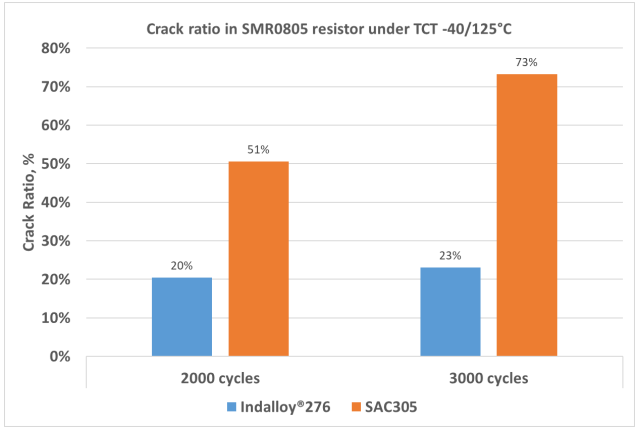

Figure 2. The crack ratio in SMR0805 resistors (on ImSn surface finish) of SAC305 and Indalloy®276 after 2000 and 3000 cycles under thermal cycling of -40/125°C.

III. Incorporation of Bismuth, Indium, and Nickle

To further improve the reliability of the SnAgCuSb based solder alloys, bismuth (Bi), Indium (In) and Nickle (Ni) are effective additives. The addition of Bi to the SnAgCuSb alloys can decrease the solidus and liquidus temperatures, thereby decreasing the reflow peak temperature. Bi also reduces the surface tension of the molten solders and improves wettability. Bi does not form any IMC precipitates with Ag, Cu, Sb or Sn. Bi, depending on the content, can strengthen the solder body through Bi particles at low temperatures and hardens the solder body through the formation of solid solutions at high temperatures. Since Bi is brittle, Bi additions beyond 4 wt.% reduce ductility significantly, although strength continues to increase. This embrittlement significantly worsens thermal fatigue resistance. Bi

continuously decreases the melting temperature with its increasing content in the solder and even forms the low melting Bi-Sn phases. These are not desired for high-temperature and high-reliability applications. Therefore, Bi addition of 1.5-3.5 wt% is preferred in the novel high-reliability lead-free solder alloys for harsh-service-environment electronics applications.

In also reduces the solidus and liquidus temperatures of solder. In is much softer than Bi and Sb, which helps to increase ductility and reduces brittleness introduced by the addition of Bi and Sb. In the novel high-reliability lead-free solder alloys with 1.5-3.5 wt% Bi and 5 to 9wt% Sb, enough In adoption minimizes the brittleness introduced by both Bi and Sb. In is prone to being incorporated into the IMC formation similar to Sn, i.e., $Ag_3(SnIn)$, $Cu_6(SnIn)_5$, $Ni_3(SnIn)_4$, and even $(CuNi)_6$ and $(SnIn)_5$, etc [1, 2]. The complicated IMC structure, requiring more atoms to diffuse towards the IMCs to continue the growth, slows down the coarsening of IMC precipitates and the thickening of interfacial IMC layers under elevated temperatures, stabilizing the joints and reducing the joint embrittlement. However, In is more prone to oxidize than Bi, which reduces wetting and increases voiding during reflow if more than 4.5wt% In is added into the solder. Thus, In addition of 4.5 wt% or below is preferred. A preferred In content in the alloy also depends on the Sb content. The addition of In strongly decreases the alloy melting temperature. To maintain high temperature performance of the joint, In addition is preferred to be less than 3.0 wt% to avoid forming these low incipient melting phases in the alloy. Table 1 summarizes the impact of each individual alloying element of Bi, Sb, and In to the Sn-Ag-Cu based solder alloys.

TABLE I. IMPACT OF INDIVIDUAL ALLOYING ELEMENT

Element	Desired Concentration	Strengthening Mechanism	Interfacial IMC formation
Sb	3.0–6.5 wt%	SS + PS(SnSb)	Slow the interfacial reaction
Bi	1.5–3.5 wt%	SS + PS(Bi)	No interfacial reaction with Cu/Ag/Ni at low concentration
In	< 3.0 wt%	SS + Partitioning into Ag(SnIn) and Cu(SnIn) IMC formation	Participate into the interfacial reaction with Cu/Ag/Ni

*SS: solid solution strengthening in Sn matrix
*PS: precipitate strengthening

The addition of small amounts of Ni (0.05-0.25 wt%) effectively improved the alloy's mechanical properties and solder joint reliability performance. During soldering, enough Ni is incorporated into the interfacial IMC formation, especially on Cu metallization, to form $(CuNi)_6Sn_5$ instead of Cu_6Sn_5. The existence of Ni inside the $(CuNi)_6Sn_5$ layer slows the IMC growth during reflow and post-reflow service, which is important to maintain interface stability and joint ductility. Ni has very limited solubility in Sn. The solder's liquidus temperature is dramatically increased when Ni is more than 0.3 wt%. Coupled with the reactivity of Ni to oxidation, the negative impacts on wetting and soldering with more than 0.3wt% Ni are observed. These effects are especially pronounced for fine powder solder paste. The interface IMC stabilization is marginal for less than 0.05 wt% Ni content due to insufficient Ni incorporation into the interfacial reaction. Therefore, 0.05-0.25 wt.% of Ni is preferred.

A solder alloy with a composition of 86.7Sn-3.2Ag-0.7Cu-5.5Sb-3.2Bi-0.5In-0.2Ni (Indalloy®292) was developed to achieve high thermal and electrical reliability based on the findings. Power cycling reliability test using HB-LED were carried out for four solder alloys (Table 2), including the commonly used SAC305.

To accelerate the power cycling test (PCT), the electrical current powering the LED was kept at a constant mode of 1A, which overloaded the LED by more than 60% (0.6A working current). Solder joint failures were evaluated in a faster way without damaging the internal wire-bond. The LED power cycler, as shown in Figure 3, was customized by the R&D team at the Indium Corporation. They are capable of testing 8 LED assemblies simultaneously. The LEDs were repeatedly powered on-and-off until failure. The power-on was carried out in a constant current mode for 8 seconds and then was powered-off for 20 seconds. Forced-air circulation was provided to continuously cool the backside of each LED assembly. The voltage, the current, and the backside temperatures of each LED assembly were recorded during power-on with a sample rate of 1Hz. Failure was identified by a sudden electrical current drop, i.e., the LED could not be powered-on anymore.

TABLE II. THE COMPOSITIONS OF SOLDER ALLOYS FOR THE LED POWER CYCLING TEST

Alloy	Sn	Ag	Cu	Sb	Bi	In	Ni
SAC305	96.5	3	0.5	--	--	--	--
276	90.6	3.2	0.7	5.5	--	--	--
276N	90.5	3.2	0.7	5.5	--	--	0.1
292	86.7	3.2	0.7	5.5	3.2	0.5	0.2

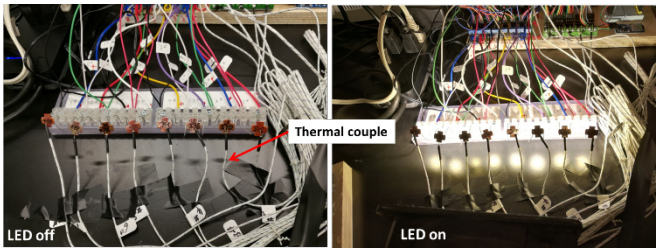

Figure 3. The LED power cycler designed by Indium Corporation. Left: power-off and Right: power-on.

Twelve LED assemblies for each alloy were made and subjected to PCT. Using a two-parameter Weibull analysis, the characteristic life (η, the number of cycles to achieve 63.2% failure N63) and slope (β) were deduced from the failure data. The results are shown in Figure 4 and summarized in Table 3. The characteristic life of Indalloy 292 nearly triples that of SAC305 (4230 cycles) and doubles that of Indalloy 276. When compared Indalloy 276 and 276N,

we find that the addition of 0.1 wt% Ni increases the characteristic life by 37%, from 6092 cycles in Indalloy 276 to 8327 cycles in 276N. The Weibull plot slopes of the four alloys were similar, as shown in Figure 4, indicating they may have a similar failure mode.

TABLE III. POWER CYCLING FAILURE WEIBULL ANALYSIS

Alloy	Slope (β)	Characteristic life (η)
SAC305	3.65	4230
276	4.52	6092
276N	4.06	8327
292	3.11	12160

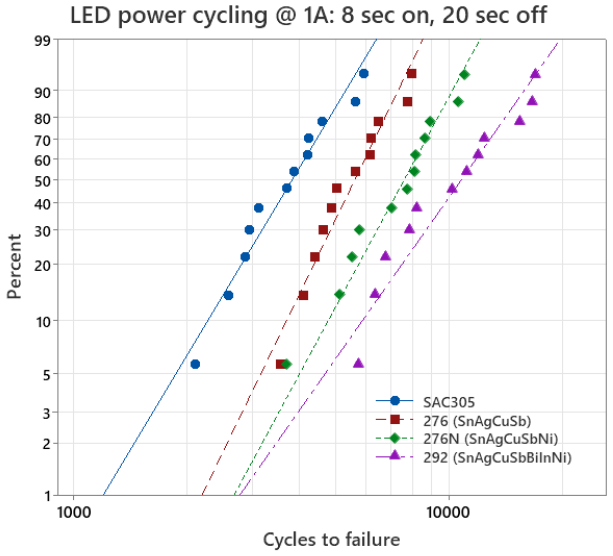

Figure 4. Weibull plot of LED power cycling reliability test

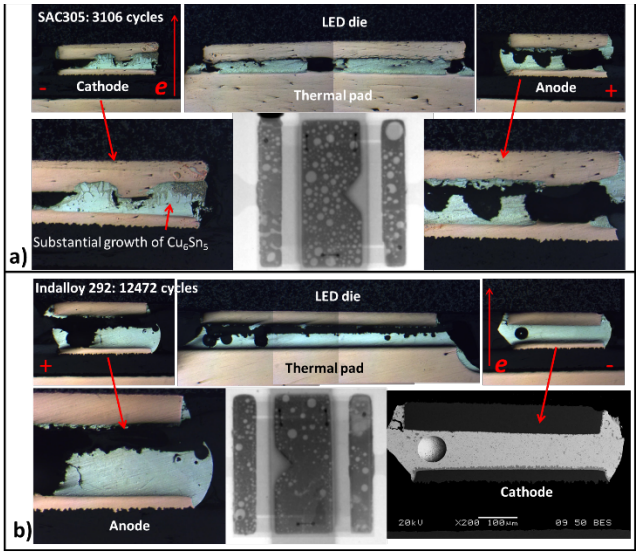

Figure 5. Optical and backscattered electron images showing the detailed microstructure of joints failed after PCTs. The X-ray image is shown in the middle. a) SAC305 failed at 3,106 cycles, b) Indalloy 292 failed at 12,474 cycles.

Figure 5 reveals the morphology of the failed joints after PCT for the SAC305 and Indalloy 292 alloys. The anode joint of SAC305 was open to fail. However, the cathode joint of SAC305 (Figure 5a, failed at 3106 cycles) had substantial growth of Cu_6Sn_5 beneath the LED chip, in which the Cu pad of the cathode joint beneath the LED chip was partially consumed, and Cu_6Sn_5 grew into the Cu pad. The growth of Cu_6Sn_5 in the thermal joint and anode did not penetrate into the Cu pads. The substantial growth of Cu_6Sn_5 and the consumption of the Cu pad were not observed in the cathode joint of Indalloy 292 but were observed in the final microstructure of the electrode joints after failure.

However, that was not the case for the thermal pad. Precipitation and growth of Cu_6Sn_5 at the cathode caused the Cu pad to be quickly consumed and resulted in a void formation at the contact area. The void reduced the contact area and displaced the electrical path, resulting in the current crowding and Joule heating inside the solder bump. Significant Joule heating inside solder joints can cause melting of the solder and quickly lead to failure. The effect of void propagation on current crowding and Joule heating was clearly seen in the X-ray images of the electrodes (Figures 5). However, this kind of Cu_6Sn_5 growth was found to be significantly slowed in the joints of Indalloy 292. This suggests the alloying of Sb, Bi, In, and Ni could effectively slow down the consumption of Cu at the electrodes, resulting in the increase of the characteristic life of the LED by 187% at 4230 cycles for SAC305 and at 12,160 cycles for Indalloy 292. Comparing Indalloy 276, 276N, and Indalloy 292 (Tables 2 and 3) indicates that adding Ni, Bi and In can further slow the consumption of Cu and enhance the reliability to both electrical current and thermal fatigue. The fundamental mechanism of the combination of positive alloying effects brought about by Sb, Bi, and In requires further investigation.

ACKNOWLEDGMENT

The authors would like to acknowledge the significant support of Christine LaBarbera on the microstructure characterization of solder joints.

REFERENCES

[1] Max Hansen, Constitution of binary alloys, 2nd edition, McGraw-Hill, 1958, pp. 1175-1177.

[2] Rodney P. Elliot, Constitution of binary alloys, First Supplement, McGraw-Hill, 1965, pp. 802.

[3] Anton-Zoran Miric, "New developments in high-temperature, high-performance lead-free solder alloys," SMTA Journal, Volume 23, Issue 4, 2010, pp. 24-29.

[4] W. Liu, N.C. Lee, "High-reliability lead-free solder alloys for harsh environment electronics applications," US Patent 11413709B2, issued August 16, 2022.

[5] J. Geng and H.W. Zhang, “A novel bismuth-, indium-, and antimony-containing lead-free solder with enhanced thermal reliability for automotive and LED applications”, Proceedings of SMTA International, 2021, pp. 805-813.

[6] J. Geng and H.W. Zhang, “Novel lead-free solder alloys based Sn-Ag-Cu-Sb with enhanced thermal and electrical reliability”, Proceedings of SMTA International, 2022, pp.333-340.

[7] Li, G.Y., Chen, B.L., Tey, J.N., “Reaction of Sn-3.5Ag-0.7Cu-xSb solder with Cu metallization during reflow soldering,” IEEE Transactions on Electronics Packaging Manufacturing, vol. 27, no. 1, 2004, pp. 77-85.

[8] Li, G.Y., Bi, X.D., Chen, Q., Shi, X.Q., “Influence of dopant on growth of intermetallic layers in Sn-Ag-Cu solder joints,” Journal of Electronic Materials, vol. 40, no. 2, 2011, pp. 165-175.

[9] Per-Erik Tegehall “Review of the impact of intermetallic layers on the brittleness of tin-Lead and lead-free solder joints, Section 3, Impact of Intermetallic Compounds on the Risk for Brittle Fractures” IVF Project Report 06/07, IVF Industrial Research and Development Corporation, 2006.

[10] S. Lu, Z. Zheng, J. Chen, F. Luo, “Microstructure and solderability of Sn-3.5Ag-0.5Cu-xBi-ySb solders,” Proceedings 11th International Conference on Electronic Packaging Technology and High-Density Packaging, ICEPT-HDP, 2010, pp. 410-412.

[11] A.A. El-Daly, Y. Swilem and A.E.Hammad, “Influences of Ag and Au additions on structure and tensile strength of Sn-5Sb lead free solder alloy,” J. Mater. Sci. Technol., vol.24, no. 6, 2008, pp. 921-925.

[12] G. E. Dieter, Mechanical Metallurgy, Chapter 6, “Dislocation theory” 159, McGraw-Hill, 1961.